

Sum-frequency generation of continuous-wave sodium D_2 resonance radiation

H. Moosmüller and J. D. Vance

Desert Research Institute, University of Nevada System, P.O. Box 60220, Reno, Nevada 89506

Received March 4, 1997

Sum-frequency generation utilizing two cw single-mode Nd:YAG lasers and a congruent lithium niobate crystal yielded 3.4 mW of very narrow-band (10 kHz over 1 ms) tunable 589-nm cw radiation. This simple solid-state light source is well suited for high-resolution spectroscopy of the sodium D_2 line, as was demonstrated with both conventional and FM-modulated saturation spectroscopy. © 1997 Optical Society of America

Tunable, single-mode lasers operating at the 589-nm sodium resonance line have been utilized in numerous scientific studies involving the sodium spectrum. Such studies commonly utilize single-mode dye lasers as narrow-band light sources. These dye lasers are very sophisticated devices that have largely been limited to laboratory use. This limitation generated interest in using solid-state lasers to generate sodium resonance radiation. An interesting coincidence of nature is that the sum frequency of two Nd:YAG laser lines, one near 1064 and one near 1319 nm, can be made resonant with the sodium D_2 line. Nd:YAG lasers have already been used for the sum-frequency generation of both relatively broadband (≈ 2 GHz) and narrow-band (≈ 150 MHz) pulsed sodium resonance radiation.¹⁻⁴ Cw sum-frequency generation is of interest because of its potential to yield very narrow-band radiation, which can be locked to sub-Doppler features of the sodium D_2 line. Such systems could, for example, replace the single-mode ring dye lasers currently used in narrow-band sodium lidar systems for atmospheric temperature and wind-velocity measurements in the mesopause region.^{5,6}

In this Letter we describe the generation of very narrow-band (10 kHz over 1 ms) cw sodium resonance radiation by type I noncritical sum-frequency mixing of the output of two cw Nd:YAG lasers in a congruent lithium niobate (LiNbO₃) crystal. This constitutes, to the best of our knowledge, the first cw solid-state source of sodium resonance radiation. Its linewidth is more than 4 orders of magnitude narrower than previous (i.e., pulsed) solid-state sources of sodium resonance radiation.

The phase-matching temperature for the sum-frequency mixing process in LiNbO₃ has been calculated from a dispersion equation⁷ to be 227.5 °C, in agreement with our experimental results. The temperature phase-matching bandwidth is relatively small (i.e., 7 °C mm), and therefore good temperature stabilization is required for our 50-mm-long LiNbO₃ crystal.

A schematic of the experimental setup for sum-frequency generation is shown in Fig. 1. Two commercially available Nd:YAG lasers, one emitting 0.7 W near 1064 nm (Lightwave Electronics Model 126-1064-700) and the other one emitting 0.35 W near 1319 nm (Lightwave Electronics Model 126-1319-350), are used

as infrared light sources. These lasers are based on a monolithic diode-pumped Nd:YAG ring cavity.⁸ Their narrow linewidth (5 kHz over 1 ms), TEM₀₀ spatial mode, and low amplitude noise (0.05% rms between 10 Hz and 10 MHz) combined with their tunability makes them well suited for the generation of very narrow-band cw sodium resonance radiation. These lasers incorporate both a relatively fast piezo tuning mechanism with 30-MHz tuning range and 30-kHz response bandwidth and a slow (1-GHz/s) thermal tuning mechanism with a tuning range of 60 GHz.⁹

The two vertically polarized laser beams are overlapped with a long-wave-pass dichroic mirror. The coaxially propagating beams are focused into a LiNbO₃ crystal with an antireflection-coated 50-mm focal-length lens, resulting in foci with Rayleigh lengths z_R of ~ 10 mm. The congruent LiNbO₃ crystal is 50 mm long by 5 mm wide by 3 mm thick, with the c axis parallel to the 50 mm \times 3 mm surface and perpendicular to the 50-mm-long edges. The front and the rear faces are tilted by 2° off normal to avoid backreflection into the laser cavities.

The LiNbO₃ crystal is held between two gold-coated copper blocks, which are heated to the phase-matching temperature (227.5 °C). Each copper block contains a heater and a temperature sensor. One of these sensors is connected to a temperature controller, which controls the current for both copper-block heaters. The current ratio between both heaters is independently set to yield nearly identical block temperatures, as determined after cross calibration of the sensors. The copper blocks together with the inserted LiNbO₃ crystal are enclosed in a Teflon block to reduce temperature fluctuations. Two small openings permit optical access to the LiNbO₃ crystal. This crystal oven

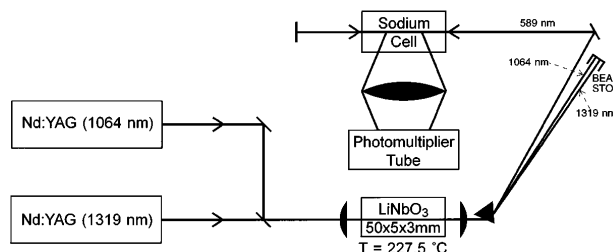


Fig. 1. Schematic diagram of the experimental setup.

has been shown to keep temporal temperature changes to less than 0.05 °C, sufficient for maintaining stable phase matching.

The sum-frequency-generated beam at 589 nm is horizontally polarized. It is collimated with an uncoated lens and separated from the infrared beams by an isosceles Brewster prism followed by a beam dump for the infrared beams. The extracted 589-nm beam is passed through a sodium cell and reflected back onto itself by a flat mirror, resulting in two counterpropagating overlapped beams in the sodium cell. This setup is used for sub-Doppler saturated fluorescence spectroscopy of the sodium D_2 line.

When the lasers were operated with their nominal output powers, the power of the generated 589-nm beam was measured to be 3.1 mW after careful optimization of beam overlap, crystal position and direction, and phase-matching temperature. This power corresponds to ~ 3.4 mW when corrected for the reflection losses of the uncoated collimation lens. To compare this experimental result with theoretical expectations, we used the theory of Boyd and Kleinman¹⁰ (BK) to write the sum-frequency power P_3 as¹¹

$$P_3 = 4\omega_1\omega_2\omega_3d_{\text{eff}}^2 \exp(-\alpha'l)P_1P_2 \frac{lh}{\pi\epsilon_0c^4n_3^2}, \quad (1)$$

where P_i are the powers, ω_i are the angular frequencies, n_i are the refractive indices of the crystal, d_{eff} is the effective nonlinear coefficient, l is the crystal length, $\alpha' = (\alpha_1 + \alpha_2 + \alpha_3)/2$, α_i are the absorption coefficients, ϵ_0 is the permittivity of vacuum, c is the speed of light in vacuum, and h is the dimensionless BK focusing factor.¹⁰ The subscripts 1, 2, and 3 refer to the 1319-, 1064-, and 589-nm beams, respectively. For noncritical phase matching, zero absorption, and foci in the center of the crystal, the BK focusing factor h can be written as¹⁰

$$h(\xi) = \frac{1}{4\xi} \left| \int_{-\xi}^{\xi} d\tau \frac{\exp(i\sigma_m\tau)}{1+i\tau} \right|, \quad (2)$$

where the focusing parameter $\xi = l/(2z_R)$ is the ratio of crystal length l and the confocal parameter $2z_R$ and σ_m is the optimum phase-matching parameter, a function of ξ . Figure 2 shows the BK focusing factor h as a function of the focusing parameter ξ . This curve is identical to the curve for no double refraction (i.e., $B = 0$) in BK's Fig. 2.¹⁰ BK's focusing factor h had a maximum of $h(\xi = 2.837) = 1.068$. However, the value of h varied quite slowly with the focusing parameter ξ , i.e., h was within 10% of its maximum for $1.56 < \xi < 5.31$.

For our experimental setup with $\xi = 2.5$ and $h = 1.063$, and relatively small absorption ($\alpha'l \ll 1$), Eq. (1) can be written as

$$P_3 = (1 - \alpha'l)\gamma l P_1 P_2, \quad (3a)$$

with

$$\gamma = \frac{4\omega_1\omega_2\omega_3h}{\pi\epsilon_0c^4n_3^2} d_{\text{eff}}^2 = (1.02 \pm 0.25)(\text{W m})^{-1}, \quad (3b)$$

where $d_{\text{eff}} = d_{31} = (5.77 \pm 0.71) \times 10^{-12}$ m/V for congruent LiNbO₃.¹² For a 50-mm-long crystal ($l = 0.05$ m) and $\alpha' = 1$ m⁻¹,^{13,14} this results in a sum-

frequency power P_3 of

$$P_3 = (0.048 \pm 0.012)\text{W}^{-1}P_1P_2. \quad (4)$$

With our lasers operating at output powers of 0.35 W at 1.319 nm and 0.7 W at 1064 nm, the laser powers coupled into the LiNbO₃ crystal were estimated to be $P_1 = 0.25$ W and $P_2 = 0.58$ W. Losses were due mainly to the Fresnel reflection on the uncoated crystal surface ($n \approx 2.2$) and the transmission loss of the dichroic mirror. This resulted in a calculated sum-frequency power of $P_3 = (7.0 \pm 1.7)$ mW inside the crystal or of (5.9 ± 1.4) mW outside the crystal after Fresnel reflection at the LiNbO₃-air interface.

The calculated power of (5.9 ± 1.4) mW was significantly larger than the measured power of 3.4 mW. This discrepancy probably was mostly due to the imperfect overlap of the infrared laser beams in the LiNbO₃ crystal. No evidence of photorefractive damage was observed, corroborating earlier experience with pulsed sum-frequency generation of 589-nm radiation in LiNbO₃.²

Our system was used to measure sub-Doppler spectra of the sodium D_2 line. Saturated absorption spectroscopy¹⁵ is commonly used for this purpose. The experimentally simpler technique of saturated fluorescence spectroscopy has found use for applications such as tuning or locking a laser, where a Doppler-broadened background causes no problem.⁵ A detailed review of saturated fluorescence spectroscopy of the sodium D lines was given recently.¹⁶ For conventional fluorescence spectroscopy, the laser beam passes through a sodium cell and the sodium fluorescence is measured with a photomultiplier tube (PMT). Recording the sub-Doppler features with saturated fluorescence spectroscopy is done with a flat mirror added behind the sodium cell (Fig. 1). The flat mirror reflects the beam back onto itself, thereby establishing the required counterpropagating beams. Our 589-nm light is wavelength tuned with the thermal tuning mechanism of one of the Nd:YAG lasers. Figure 3 shows a saturated fluorescence spectrum recorded with this simple setup and our new light source. The three narrow-band sub-Doppler features are clearly visible.

With the simple addition of a lock-in amplifier for processing the PMT signal, frequency-modulated

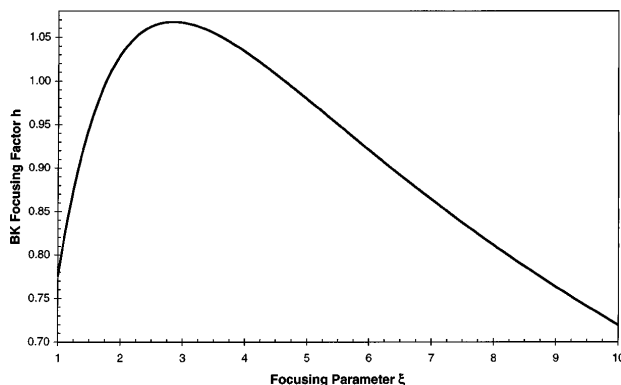


Fig. 2. BK focusing factor h as a function of the focusing parameter ξ .

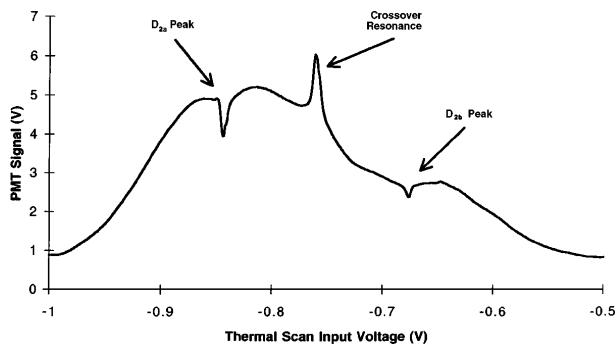


Fig. 3. Saturated fluorescence spectrum of the sodium D_2 line, showing sub-Doppler features at the D_{2a} peak, the D_{2b} peak, and the crossover resonance.

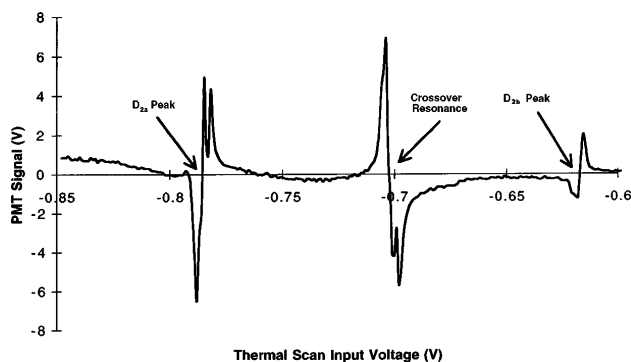


Fig. 4. Frequency-modulated saturated fluorescence spectrum of the sodium D_2 line, showing sub-Doppler features at the D_{2a} peak, the D_{2b} peak, and the crossover resonance.

saturated fluorescence spectroscopy can be implemented.¹⁷ The reference sine-wave output of the lock-in amplifier is used as input to the fast piezo tuning of one of the Nd:YAG lasers. Amplitude and frequency of the frequency modulation were near 3 MHz and 1 kHz, respectively. The resulting frequency-modulated spectrum, essentially a derivative of the conventional spectrum, is shown in Fig. 4. The Doppler-broadened background is strongly suppressed, while the narrow Doppler-free features are enhanced. The center of the sub-Doppler feature is characterized by the zero

crossing of the signal, which makes it ideally suited for frequency-locking purposes.

In conclusion, more than 3 mW of very narrow-band tunable cw sodium D_2 resonance radiation has been generated by sum-frequency generation in congruent lithium niobate.

It is a pleasure to acknowledge helpful discussions with Peter Bordui, Dave Gerstenberger, Tom Jeys, Greg Mizell, and Joe She. This research was supported in part by National Science Foundation grant ATM 9402166 and ATM 9612823.

References

1. C. G. Bethea, *IEEE J. Quantum Electron.* **QE-9**, 254 (1973).
2. T. H. Jeys, A. A. Brailove, and A. Mooradian, *Appl. Opt.* **28**, 2588 (1989).
3. R. W. Farley and P. D. Dao, *Appl. Opt.* **34**, 4269 (1995).
4. P. H. Chiu, A. Magana, and J. Davis, *Opt. Lett.* **19**, 2116 (1994).
5. C. Y. She, H. Latifi, J. R. Yu, R. J. Alvarez II, R. E. Bills, and C. S. Gardner, *Geophys. Res. Lett.* **17**, 929 (1990).
6. C. Y. She and J. R. Yu, *Geophys. Res. Lett.* **21**, 1771 (1994).
7. G. J. Edwards and M. Lawrence, *Opt. Quantum Electron.* **16**, 373 (1984).
8. T. J. Kane and R. L. Byer, *Opt. Lett.* **10**, 65 (1985).
9. Lightwave Electronics, "Specifications of the series 126 diode-pumped non-planar ring laser," (Lightwave Electronics, Mountain View, Calif., 1994).
10. G. D. Boyd and D. A. Kleinman, *J. Appl. Phys.* **39**, 3597 (1968).
11. K. Sugiyama, J. Yoda, and T. Sakurai, *Opt. Lett.* **16**, 449 (1991).
12. M. M. Choy and R. L. Byer, *Phys. Rev. B* **14**, 1693 (1976).
13. Y. C. See, S. Guha, and J. Falk, *Appl. Opt.* **19**, 1415 (1980).
14. P. F. Bordui, Crystal Technology, Inc., Palo Alto, Calif., 94303 (personal communication, 1994).
15. T. W. Hänsch, I. S. Shahin, and A. L. Schawlow, *Phys. Rev. Lett.* **27**, 707 (1971).
16. C. Y. She and J. R. Yu, *Appl. Opt.* **34**, 1063 (1995).
17. G. C. Bjorklund, *Opt. Lett.* **5**, 15 (1980).